Acoustic impedance measurements of pulse tube refrigerators

Takashi Iwase,[1] Tetsushi Biwa,[1,a)] and Taichi Yazaki[2]
[1]*Department of Mechanical Systems and Design, Tohoku University, Sendai 980-8579 Japan*
[2]*Department of Physics, Aichi University of Education, Kariya 448-8542, Japan*

(Received 26 October 2009; accepted 26 December 2009; published online 3 February 2010)

Complex acoustic impedance is determined in a prototype refrigerator that can mimic orifice-type, inertance-type, and double inlet-type pulse tube refrigerators from simultaneous measurements of pressure and velocity oscillations at the cold end. The impedance measurements revealed the means by which the oscillatory flow condition in the basic pulse tube refrigerator is improved by additional components such as a valve and a tank. The working mechanism of pulse tube refrigerators is explained based on an electrical circuit analogy. © *2010 American Institute of Physics*. [doi:10.1063/1.3296225]

I. INTRODUCTION

The first pulse tube refrigerator, what we now call a *basic pulse tube refrigerator*, was developed in the mid 1960s.[1] It was named after the use of a "pulse tube," which is a closed tube located next to a regenerator, as presented in Fig. 1(a). Merely by introducing pulsating gas flows into the pulse tube through the regenerator, the temperature at the junction of these parts decreased to 199 K. Its simple structure presents remarkable advantages over other regenerative refrigerators such as Stirling and Gifford–McMahon refrigerators, but the lowest attainable temperature was higher than those of the others were.

In 1984, two decades after the invention of the pulse tube refrigerator, Mikulin *et al.*[2] developed an *orifice pulse tube refrigerator* (OPTR), presented in Fig. 1(b), by installing an orifice and a buffer tank near the warm end of the pulse tube. They succeeded thereby in lowering the temperature to 105 K. In 1990, Zhu *et al.*[3] introduced a bypass that connected the hot end of the regenerator and that of the pulse tube of the OPTR. The developed *double inlet pulse tube refrigerator* (DIPTR) achieved a temperature of 25 K. Since then, various pulse tube refrigerators have been developed including an *inertance pulse tube refrigerator* (IPTR).[4] Figures 1(c) and 1(d) portray the IPTR and the DIPTR, respectively. In recent pulse tube refrigerator designs, temperatures even below the condensation point of helium are attainable,[5] although the pulse tube refrigerator has no moving parts at the cold end.

A key to the improvement of pulse tube refrigerators is the phase difference Φ between pressure oscillation $P=p\exp\{i(\omega t+\Phi)\}$ and cross-sectional mean velocity oscillation $U=u\exp(i\omega t)$ at the cold end of the refrigerator,[6–8] $\Phi\sim-90°$ in the basic pulse tube refrigerator, whereas $-90°<\Phi<0°$ in the OPTR.[9] In the modern pulse tube refrigerators such as the DIPTR and the IPTR, Φ satisfies the relation $\Phi>0°$,[10,11] which assures a flow condition equivalent to that in the Stirling and Gifford–McMahon refrigerators.[12] However, the ability to control Φ has not been addressed experimentally through direct measurements of P and U.

In this study, we constructed a prototype pulse tube refrigerator that can mimic OPTR, DIPTR, and IPTR, as well as the basic pulse tube refrigerator. We experimentally determine the complex acoustic impedance Z

$$Z=\frac{P}{AU}, \tag{1}$$

at the cold end of the pulse tube through simultaneous measurements of P and U, where AU represents the volume velocity. The phase of Z is equal to the phase lead of P to U. The magnitude represents the amplitude ratio of P to U, which is also the key factor determining the cooling performance of the refrigerator. Results show that the experimental acoustic impedance clearly explains drastic changes of the gas dynamics that are responsible for improvement of the pulse tube refrigerator. The role of the components of the pulse tube refrigerators is also identified based on an electrical circuit analogy.

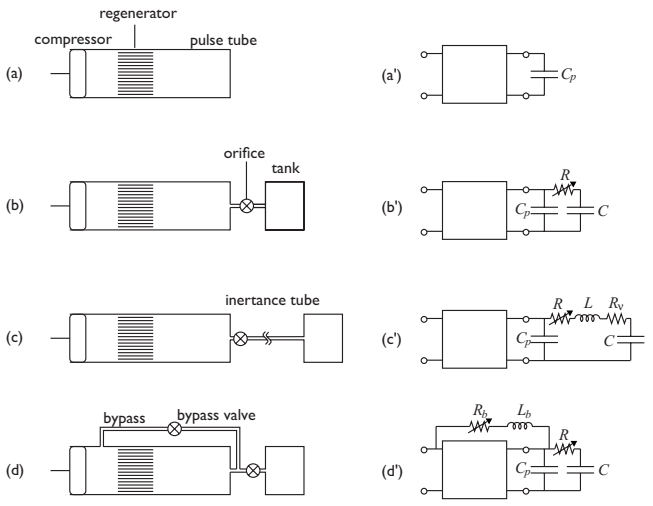

FIG. 1. Pulse tube refrigerators: (a) basic, (b) orifice, (c) inertance, and (d) DIPTR. Panels (a′)–(d′) present the corresponding equivalent electrical circuits.

[a)]Electronic mail: biwa@amsd.mech.tohoku.ac.jp.

II. LUMPED IMPEDANCE MODEL

A lumped impedance model analogous to an electrical circuit can provide an intuitive understanding of the phasing[13,14] within a framework of the linear acoustic theory.[15] In this model, the oscillating pressure corresponds to ac electrical voltage; the oscillating volumetric velocity corresponds to ac electrical current. The compliance C of a *wide* tube with volume V, analogous to an electrical capacitor, is

$$C = K_S V, \tag{2}$$

where $K_S = 1/(\gamma p_m)$ denotes the adiabatic compressibility of the gas, γ is the specific heat ratio, and p_m is the mean pressure. Adiabatic compressibility K_S is usually a good approximation for the gas in a buffer tank because the tank's diameter is much greater than the thermal penetration depth δ of the gas, where δ is given as $\delta = \sqrt{2\alpha/\omega}$ using thermal diffusivity α of the gas. However, it fails when the tube diameter is not sufficiently large for the gas to undergo thermodynamically adiabatic processes. Such is the case for the pulse tube used for this study, in which the compressibility of the gas differs from K_S as we show later.

The inertance L and the resistance R_v of a *narrow* tube with length l and cross-sectional area A, analogous to an electrical inductance and resistor, are expressed, respectively, as

$$L = \frac{\rho_m l}{A}, \tag{3}$$

$$R_v = \frac{8\pi\nu l}{\rho_m A^2}, \tag{4}$$

where ρ_m is the mean density and ν is the kinematic viscosity of the gas. The orifice is taken as a resistor whose resistance changes as it opens. Based on experimental results, we will present the resistance of the orifice valve in this study.

Figures 1(a′)–1(d′) present the electrical circuit equivalent to the pulse tube refrigerators shown in Figs. 1(a)–1(d). The combined impedance of the components at the right-hand side of the regenerator is given as

$$\frac{1}{Z} = i\omega C_p + \frac{i\omega C}{1 + i\omega RC}, \tag{5}$$

for the OPTR, and

$$\frac{1}{Z} = i\omega C_p + \frac{i\omega C}{1 - \omega^2 LC + i\omega R'C}, \tag{6}$$

for the IPTR, where C_p denotes the compliance of the pulse tube, and $R' = R + R_v$ is the sum of resistance of the valve and the inertance tube. In contrast to the arrangement of acoustical elements in OPTR and IPTR in series, the DIPTR is equipped with a bypass tube that is aligned in parallel to the pulse tube. This arrangement obscures the analytical expression of Z because the equivalent electrical elements are unknown for the complicated flow channels in the regenerator and heat exchangers. We experimentally verify Z in Eqs. (5) and (6), and propose the equivalent circuit model for the regenerator assembly in this study.

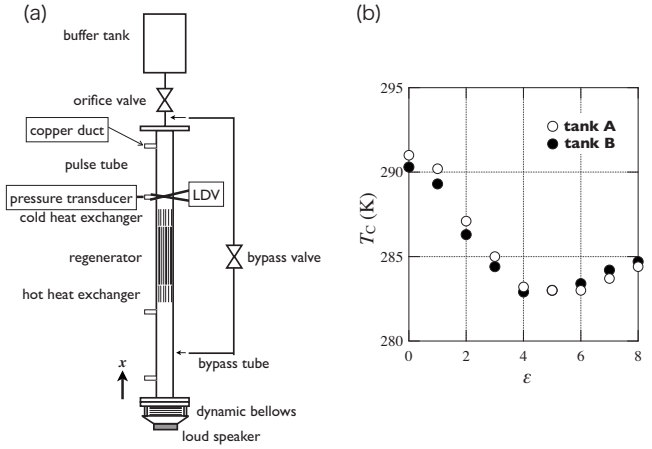

FIG. 2. Schematic illustration of the present OPTR prototype (a). Cooling temperature of the OPTR as a function of the turns ϵ.

III. EXPERIMENT

A. Prototype pulse tube refrigerators

Figure 2(a) schematically depicts the OPTR used in this experiment. A woofer speaker connected with dynamic bellows was used as a compressor to produce periodic gas oscillations. A regenerator consisting of stacked stainless-steel screen meshes was sandwiched between hot and cold heat exchangers. The mesh number per inch is 250, the wire diameter d_w is 0.04 mm. The regenerator length and its internal diameter were, respectively, 50 and 15 mm. Heat exchangers were made of 1-mm-thick brass plates aligned in parallel with spacing of 0.5 mm separating them. A 60-mm-long glass cylinder with internal diameter of 13.4 mm was used as a pulse tube. An 80-mm-long glass cylinder was situated between the regenerator and the compressor.

A needle valve (B-2MG-MH; Swagelok Co.) was placed as an adjustable orifice between the hot end of the pulse tube and a buffer tank. Its opening is expressed by the number ϵ of turns ($0 \le \epsilon \le 8$), the valve is fully open when $\epsilon = 8$, although it is closed when $\epsilon = 0$. We used cylindrical buffer tanks of two types: one has internal volume of 0.483×10^{-4} m^3 (tank A) and the other has internal volume of 5.28×10^{-4} m^3 (tank B). When the valve is closed, the prototype works as the basic pulse tube refrigerator; although it operates as the OPTR when the valve is open. The IPTR and the DIPTR are constructed by modifying the OPTR, as we will describe later.

B. Cooling performance of the OPTR

Prior to measurements of oscillatory flows, we tested the cooling performance of the present OPTR. For operation at high amplitudes, the woofer speaker unit was replaced with a rotary valve connected to a gas cylinder filled with pressurized nitrogen via a regulator. The rotary valve switched periodically to the OPTR and a vent port. It thereby provided pressure oscillations into the OPTR. The working frequency was adjusted at 5.9 Hz. The maximum excess pressure from the mean pressure (100 kPa) was about 20 kPa in the pulse tube.

Figure 2(b) presents the cooling temperature T_C of the OPTR when ϵ is changed from 0 to 8. The temperature T_C shows a minimum at $\epsilon=4$ for tank A, whereas the lower minimum T_C was obtained with $\epsilon=6$ for tank B. Presence of the optimum ϵ is commonly observed in the OPTR. Consequently, our prototype fundamentally performs the same function as those in practical devices.

C. Measurements of acoustic impedance

The acoustic pressure $P=p\exp\{i(\omega t+\Phi)\}$ was measured using small pressure transducers via small ducts with 2 mm internal diameter and 10 mm length. At the same axial position, the axial acoustic particle velocity was measured on the central axis of the tube using a laser Doppler velocimeter (Flowlite, Dantec Dynamics AS). Cigarette smoke was introduced into the glass tubes through the small ducts to serve as seeding particles. The measured central velocity was converted to the cross-sectional mean velocity $U=u\exp(i\omega t)$ using the theoretical result of the laminar flow theory.[16] The complex acoustic impedance was determined as

$$Z=\frac{p}{Au}e^{i\Phi}, \tag{7}$$

where $-\pi<\Phi<\pi$. The measured Z will be shown as a phasor in the complex plane in the following sections.

The working fluid is air at atmospheric pressure. The driving voltage supplied to the woofer speaker was controlled using a function generator. The driving frequency was kept at $f=5.9$ Hz; the amplitude was fixed such that the acoustic pressure was $p=1.1$ kPa in the pulse tube when the orifice valve was closed ($\epsilon=0$).

IV. RESULTS AND DISCUSSION

A. Basic pulse tube refrigerators and OPTR

Acoustic variables P and U were observed to vary as functions of axial coordinate x and turns ϵ of the orifice valve. Here, the origin of axial coordinate x was taken at the top flange of the woofer speaker, and directed toward the upper glass cylinder. We specifically examine the ϵ dependence of the complex acoustic impedance Z at the duct position ($x=170$ mm) nearest the cold end of the prototype. Solid circles in Fig. 3 represent the experimental Z measured for the OPTR with the tank A. Numbers in the figure represent the turns ϵ of the valve.

When the orifice valve is closed ($\epsilon=0$), Z is positioned very closely to the imaginary axis on the complex plane. Therefore, the phase Φ of pressure P relative to velocity U is close to a standing wave phase (=−90°) in the basic pulse tube refrigerator.[6] As ϵ increases, Z traces a semicircle in a counterclockwise direction. A maximum of Φ (=−44.6°) is achieved with $\epsilon=4$ corresponding to a minimum temperature obtained in the cooling test [Fig. 2(b)]. The impedance Z for tank B shows the maximum $\Phi=-11.6°$ when $\epsilon=6$, which also gives the minimum cooling temperature. These results indicate that the orifice valve controls the cooling performance of the OPTR by tuning Φ at the cold end of the regenerator.

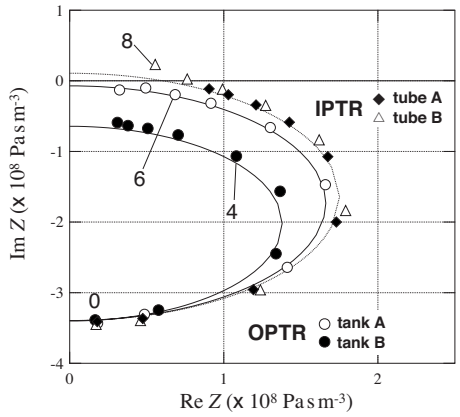

FIG. 3. Complex acoustic impedance Z of the OPTR and the IPTR. Numbers refer to the turn ϵ of the orifice valve. Solid and dotted curves represent Z of the equivalent circuits.

Based on results of experimental Z, let us determine the two constants appearing in the lumped impedance model presented in Fig. 1(b′), one is the compliance C_p of the pulse tube. The other is the variable resistance R of the orifice valve. The compliance C of the tank was obtained from Eq. (2). After some algebraic calculation, the impedance Z in Eq. (5) turns out to draw a semicircle when the resistance R is chosen as a parameter; Z goes to $1/i\omega(C_p+C)$ when $R=0$; it goes to $1/(i\omega C_p)$ when R becomes infinity. Unknown compliance C_p of the pulse tube was determined from the experimental Z when $\epsilon=0$, which gave the effective compressibility K of the gas in the pulse tube region as $K=8.95\times10^{-6}$ Pa^{-1}. The relation $K_T<K<K_S$ (where $K_T=1/p_m$ is the isothermal compressibility of the gas) means that the gas undergoes intermediate thermodynamic processes between adiabatic and isothermal ones. This is reasonable because the ratio of the tube radius to thermal penetration depth of the gas is 6.3 in the pulse tube.

Comparison of the experimental and the model impedances also enables us to estimate the resistance R of the valve, as portrayed in Fig. 4. It is apparent that the inverse of resistance (conductance) of the present valve monotonically increases concomitantly with increasing ϵ. Results show that the conductance is proportional to the flow coefficient provided by the valve manufacturer (Swagelok Co.). Validity of the equivalent circuit is also supported by the mutual agreement of R obtained using tanks A and B, and also with the IPTR.

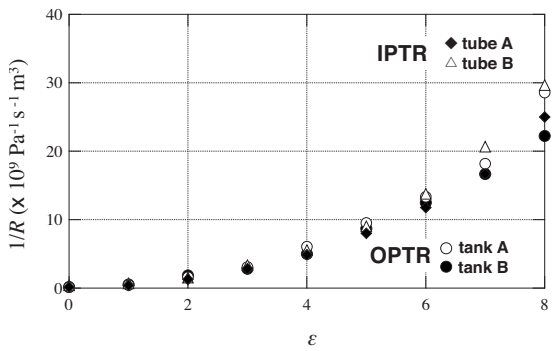

FIG. 4. Inverse of the resistance R as a function of the turns ϵ of the orifice valve.

Before ending this section, the shortcomings of OPTR must be noted. First, the phase Φ never becomes positive. The semicircle drawn by the impedance Z remains in the fourth quadrant, as depicted in Fig. 3, although the increase of the compliance moves it close to the first quadrant. Second, the increase of viscous and thermal losses in the regenerator is unavoidable because $|Z|$ tends to zero when one attempts to make Φ to be close to zero by the large compliance. The high acoustic impedance $|Z|$ with positive Φ is required for the pulse tube refrigerator working competitively with the Stirling refrigerator. The IPTR and the DIPTR provide some examples to achieve such a flow condition, as we show below.

B. IPTR

The IPTR might be regarded as a simple extension of the OPTR. Only a long tube makes the IPTR different from the OPTR. We modified the OPTR prototype into the IPTR by installing an inertance tube (tube A) with length $l=1.2$ m and internal diameter $d=2$ mm between the orifice valve and the buffer tank. The orifice valve was used to control the resistance independently of the inertance. We used tank B in the IPTR prototype.

Considering the inertance L, the equivalent circuit is expressed as presented in Fig. 1(c′). Equation (6) gives the corresponding impedance, which is depicted in Fig. 3 as dots. Here the inductance L was calculated using Eq. (3); the total resistance $R'(=R+R_v)$ was taken as a variable parameter changing from infinity to zero. The model impedance traces a semicircle entering the first quadrant when R' approaches zero. Figure 3 also portrays the experimental Z measured at the cold end of the pulse tube in the IPTR. Good agreement is apparent between the experimental and the model impedances Z, although the experimental Z remains in the fourth quadrant without reaching the first.

To obtain the positive Φ, we used tube B having $l=5$ m and $d=4$ mm in place of tube A. Tube B provides the same inertance L with less the resistance R_v. Figure 3 shows that the impedance Z of the IPTR with the modified inertance tube goes into the first quadrant when $\epsilon \geq 7$. Realization of positive Φ, as in the Stirling cooler, is the advantage of the IPTR over the OPTR. It is noteworthy, however, that use of the inertance tube does not always yields positive Φ, as we describe below.

Presuming that L and R' can be adjusted independently of each other, when R' is infinitely large, the impedance in Eq. (6) decreases to $Z_\infty = 1/(i\omega C_P)$. It becomes

$$Z_0 = \frac{1-\omega^2 LC}{i\omega(C_P + C - \omega^2 L C_P C)}, \tag{8}$$

when R' goes to zero. As R' decreases to zero, the impedance Z traces a semicircle extending from Z_∞ to Z_0, as depicted in Fig. 3. Only when L satisfies

$$\frac{1}{\omega^2 C} < L < \frac{C_P + C}{\omega^2 C_P C}, \tag{9}$$

does the phase Φ of Z become positive with appropriate R'. In other cases, Z stays within the fourth quadrant, irrespective of R'. In the OPTR, the larger compliance always results in the larger Φ when the variable resistance is suitably adjusted. In the IPTR, however, one must choose adequate L and R' to achieve Φ best suited for the thermoacoustic cooling effect. Use of the orifice valve is useful for finding the adequate resistance R' for a given L and C because we can control R' independently of L. Once R' that gives the proper phasing is found, the inertance tube and the valve can be replaced with a new inertance tube such that the l/A value is retained to keep L constant, whereas the l/A^2 value is increased from that of the original inertance tube to increase R_v.

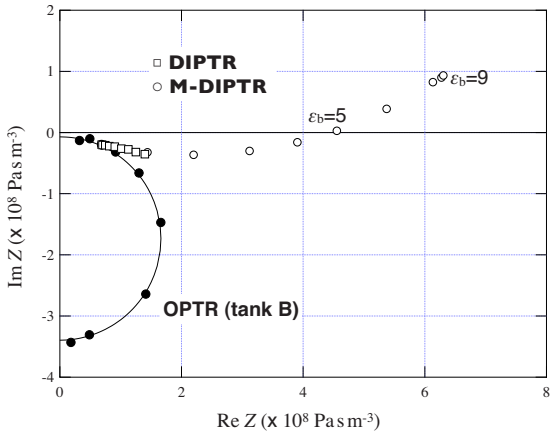

FIG. 5. (Color online) Complex acoustic impedance Z of the DIPTR and the modified one when the turns ϵ of the orifice valve are 6. Numbers refer to the turn ϵ_b of the double inlet valve. Solid circles represent the data of the OPTR reproduced from Fig. 3.

C. DIPTR

The OPTR was modified to the DIPTR using a bypass tube with length $l=300$ mm and internal diameter $d=2$ mm and a bypass valve (B-2MG-MH; Swagelok Co.). One end of the bypass tube was connected to the glass tube at $x=44$ mm, and the other end to the short tube between the orifice valve and the pulse tube, as presented in Fig. 2(a). Opening the bypass valve turns the OPTR into the DIPTR.

Figure 5 presents the experimental acoustic impedance Z of the DIPTR at the cold end of the pulse tube. Starting from the optimum point of the OPTR ($\epsilon=6$), the phasor Z goes linearly away from the origin with opening the bypass valve. Although the magnitude of Z increases monotonically, the phase difference Φ between P and U remains at the optimum in the OPTR.

To elucidate the effect of the double inlet configuration further, we increased d of the bypass tube to 4 mm and replaced the bypass valve with that having the larger conductance ($0 \leq \epsilon_b \leq 9$, SS-1RS4; Swagelok Co.). This made the bypass flow conductance 10 times larger than that of the original one. The impedance Z of the modified DIPTR shows the arc going into the first quadrant when $\epsilon_b \geq 5$, as presented in Fig. 5 by circles. It is noteworthy that the magnitude of Z with $\epsilon_b=5$ is much larger than that of the IPTR with the same phasing $\Phi=0$. This result verifies that the DIPTR can achieve both a desired phasing and very high acoustic impedance.

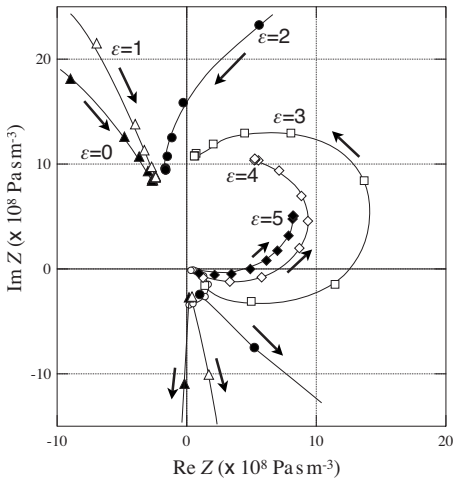

FIG. 6. Complex acoustic impedance Z of the modified DIPTR when the turns ϵ of the orifice valve are varied from 5 to 0. Curves are a guide to the eye. The impedance Z changes in the direction of the arrows as ϵ_b increases.

Experimental results with $\epsilon \leq 5$ are depicted in Fig. 6. Very large arcs are depicted in the first quadrant on the complex plane, which suggests that both $|Z|$ and Φ are extremely sensitive to small changes of ϵ and ϵ_b. This might add some instability to the DIPTR, as well as the acoustic streaming.[17] Specifically with $\epsilon \leq 2$, negative Re Z was observed. The sign of Re Z represents the flow direction of the acoustic work flow I, equivalent to the acoustic power flux per unit area, given as

$$I = \frac{1}{2} pu \cos \Phi = \frac{1}{2} (\mathrm{Re}\, Z) u^2. \tag{10}$$

Although positive I represents the flow through the regenerator to the pulse tube, negative I means that I oppositely flows into the regenerator from the pulse tube side. Negative Re Z was also found at $x=76$ mm in the driver side of the regenerator. Therefore, I passes through the regenerator from top to bottom, oppositely to I in the ordinary pulse tube refrigerators. In other words, I supplied from the acoustic driver circulates through the bypass line and the regenerator. Such a pulse tube refrigerator can have a high thermal efficiency, especially at moderate cooling temperatures, because it can recover the acoustic power that is lost in the ordinary pulse tube refrigerators.[18]

D. Equivalent circuit of regenerator

We determine here the equivalent circuit of the regenerator based on the measured oscillatory pressure and velocity at ends of the regenerator. In this experiment, the temperature gradient is absent along the regenerator, which enables us to express the equivalent circuit as portrayed in Fig. 7. The pressure P_1 and the volumetric velocity AU_1 at the bottom of the regenerator ($x=76$ mm) is related to P_2 and AU_2 at the top ($x=170$ mm) as

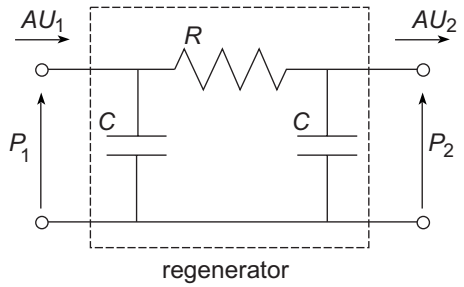

FIG. 7. Equivalent electrical circuit of the regenerator without the temperature gradient.

$$\begin{pmatrix} P_1 \\ AU_1 \end{pmatrix} = \begin{pmatrix} 1 + i\omega RC & R \\ -\omega^2 C^2 [R + 2/(i\omega C)] & 1 + i\omega RC \end{pmatrix} \begin{pmatrix} P_2 \\ AU_2 \end{pmatrix}. \tag{11}$$

Solving Eq. (11) with respect to R and C, and inserting the experimental P_i, AU_i $(i=1,2)$ into it yields $R=[4.6\pm0.1 + i(-0.060\pm0.003)]\times10^7$ Pa s m^{-3}, and $C=[3.1\pm0.1 + i(0.60\pm0.01)]\times10^{-11}$ m^3/Pa. In all, we used 24 sets of P_i and AU_i obtained for the OPTRs (with tanks A and B) and the DIPTR with various valve settings. The validity of the proposed circuit is assured by the relations Re $R \gg$ Im R and Re $C \gg$ Im C.

From the obtained R and C, we estimate the effective pore diameter and the effective compressibility in flow passages of the present regenerator. Presuming that the regenerator is regarded as a bundle of cylindrical pores with effective diameter d_{eff}, the resistance R of the regenerator is expressed as

$$R = \frac{R_h}{N}, \tag{12}$$

where $R_h = 8\pi\mu l / A_h^2$ represents the flow resistance of a single pore with cross-sectional area $A_h = \pi d_{\mathrm{eff}}^2/4$ and length l, $N = \psi(D/d_{\mathrm{eff}})^2$ denotes the number of pores given by the internal diameter D of the regenerator housing ($D=15$ mm), and ψ is the porosity that was determined experimentally as 72% for the present regenerator. Inserting the experimental $R = 4.6\times10^7$ Pa s m^{-3} into Eq. (12), we obtain $d_{\mathrm{eff}} = 0.070$ mm. This is 30% smaller than the hydraulic diameter of the regenerator that is given as $\psi d_w/(1-\psi) = 0.1$ mm, where d_w is the wire diameter of screen meshes.[7] It is noteworthy that the pore diameter d agrees well with the empirical diameter $D_{\mathrm{eff}}=0.064$ mm given as

$$D_{\mathrm{eff}} = \sqrt{D_h d_w}, \tag{13}$$

that Ueda *et al.*[19] proposed.

The compliance C of the regenerator is expressed as

$$C = \psi K V/2, \tag{14}$$

where V ($=D^2L/4$, L is the axial length of the regenerator) denotes the internal volume of the regenerator housing, and where K is the effective compressibility of the gas. The factor 1/2 is added because of the two capacitors in the equivalent circuit in Fig. 7. Inserting the experimental C yields $K = 0.98\times10^{-5}$ 1/Pa, which shows good agreement with the isothermal compressibility $K_T = 1/p_m = 1.0\times10^{-5}$ 1/Pa.

Therefore, the gas oscillates isothermally in the regenerator. The equivalent circuit for the present model is at least verified when the temperature gradient is absent. It would give a first step for modeling a practical regenerator working at cryogenic temperatures.

V. SUMMARY

We built a prototype pulse tube refrigerator and determined the complex acoustic impedance Z at the cold end of the pulse tube through simultaneous measurements of P and U. The OPTR is superior to the basic pulse tube refrigerator because of the controllability of the phasing Φ in the region $-90° < \Phi < 0°$. Further improvement is achieved by the DIPTR and the IPTR because they can achieve positive Φ and increase the magnitude of Z. These characteristic changes explain the successive improvements of cooling performance achieved by these pulse tube refrigerators.

In this study, the acoustic impedance of the pulse tube refrigerators was found to be controlled similarly to the electrical impedance in the electrical circuit. The electrical circuit analogy is a powerful tool to predict the oscillatory flow dynamics in pulse tube refrigerators. It is important to verify the analogy's validity in high-amplitude flows and in the presence of a large temperature gradient along the regenerator.

[1]W. E. Gifford and R. C. Longsworth, ASME J. Eng. Ind. **63**, 264 (1964).
[2]E. I. Mikulin, A. A. Tarasov, and M. P. Shkrebyonck, Adv. Cryog. Eng. **29**, 629 (1984).
[3]S. Zhu, P. Wu, and Z. Chen, Cryogenics **30**, 514 (1990).
[4]K. Kanao, N. Watanabe, and Y. Kanazawa, Cryogenics **34**, 167 (1994).
[5]C. Wang, G. Thummes, and C. Heiden, Adv. Cryog. Eng. **43**, 2055 (1988).
[6]A. Tominaga, Cryogenics **35**, 427 (1995); A. Tominaga, *Fundamental Thermoacoustics* (Uchida Roukakuho, Tokyo, 1998).
[7]G. W. Swift, *Thermoacoustics: A Unifying Perspective for Some Engines and Refrigerators* (Acoustical Society of America, Sewickley, 2002).
[8]G. W. Swift, J. Acoust. Soc. Am. **84**, 1145 (1988).
[9]R. Radebaugh, Adv. Cryog. Eng. **35**, 1191 (1990).
[10]A. Tominaga, Teion Kougaku **27**, 146 (1992).
[11]A. Hofmann and H. Pan, Cryogenics **39**, 529 (1999).
[12]S. Sunahara, T. Biwa, and U. Mizutani, J. Appl. Phys. **92**, 6334 (2002).
[13]D. L. Gardner and G. W. Swift, Cryogenics **37**, 117 (1997).
[14]A. Tominaga and T. Haruyama, Teion Kougaku (in Japanese) **31**, 267 (1996).
[15]L. E. Kinsler, A. R. Frey, A. B. Coppens, and J. V. Sanders, *Fundamentals of Acoustics*, 4th ed. (Wiley, New York, 2000).
[16]T. Biwa, Y. Ueda, H. Nomura, U. Mizutani, and T. Yazaki, Phys. Rev. E **72**, 026601 (2005).
[17]D. Gedeon, Cryocoolers **9**, 385 (1997).
[18]G. W. Swift, D. L. Gardner, and S. Backhaus, J. Acoust. Soc. Am. **105**, 711 (1999).
[19]Y. Ueda, T. Kato, and C. Kato, J. Acoust. Soc. Am. **125**, 780 (2009).